coatings

MDPI

Article

Development of Antimicrobial Microcapsules of Saffron Petal Essential Oil by Condensation Method and Its Excellent Binding on Cotton Fibers

Su Liu [1], Liuxin Shi [1,*], Mengyun Liu [1], Wei Chen [1], Qiang Cheng [2] and Xiuli Song [1]

[1] College of Light Industry and Food Engineering, Nanjing Forestry University, Nanjing 210037, China; liusu@njfu.edu.cn (S.L.); 13093313363@163.com (M.L.); cww@njfu.edu.cn (W.C.); songxiuli@njfu.edu.cn (X.S.)
[2] College of Forestry, Nanjing Forestry University, Nanjing 200137, China; chengqiang@njfu.edu.cn
* Correspondence: shiliuxin@njfu.edu.cn; Tel.: +86-25-85428859

Abstract: In recent years, textiles with antimicrobial properties have attracted more and more attention. As natural antimicrobial agents, essential oils' potential application value lies in their ability to provide textiles with antimicrobial functions. In this paper, organic solvent extraction (n-hexane, petroleum ether, ethanol) and steam distillation were used to extract saffron petal essential oil (SPEO). It was found that organic solvent extraction (ethanol) had the highest extraction rate and the most apparent bacteriostatic effect. SPEO-Ms were prepared using the composite condensation method with gelatin and chitosan. The microstructure, encapsulation efficiency, slow-release performance, infrared spectrum, and thermal stability of the SPEO-Ms were evaluated. The results showed that the microencapsulated essential oil had good bacteriostatic properties. Antimicrobial cotton fabric was prepared by impregnating microcapsules onto cotton fibers. The effects of the microcapsules' concentration on the whiteness, air permeability, moisture permeability, and bacteriological inhibition of the fabric were investigated. The results revealed that SPEO-Ms have the potential to be used as a new antimicrobial agent in textiles.

Keywords: saffron flower petal essential oil; microcapsule; antimicrobial cotton fabric; cotton fabric

Citation: Liu, S.; Shi, L.; Liu, M.; Chen, W.; Wang, M.; Cheng, Q.; Song, X. Development of Antimicrobial Microcapsules of Saffron Petal Essential Oil by Condensation Method and Its Excellent Binding on Cotton Fibers. *Coatings* **2023**, *13*, 714. https://doi.org/10.3390/coatings13040714

Academic Editor: Eleftherios G. Andriotis

Received: 1 March 2023
Revised: 17 March 2023
Accepted: 20 March 2023
Published: 31 March 2023

1. Introduction

Plant-based essential oil is a kind of natural high-concentration extract obtained by the distillation or physical pressing of plant roots, skins, fruits, seeds, flowers, and leaves. These essential oils are mainly composed of volatile organic compounds with a low molecular weight and have been shown to have environmentally protective characteristics [1]. The various compounds contained in them possess therapeutic properties, including antimicrobial, antioxidant, anti-inflammatory, and antiviral effects [2,3]. As a result, essential oil is often used in preservation and anticorrosion applications and is also employed in the chemical, medicine, and health-care industries [4,5]. Different types of essential oils have been studied around the world, including those from basil [6], rose [7], cinnamon [8], thyme [9], cloves [10], and saffron [11–14].

Studies of saffron mainly focus on its stigma, which only accounts for 7.4% of the whole flower [15]. There are few studies on saffron petal essential oil. Up to the present, studies on saffron flower petal essential oil have mainly focused on its antioxidant [16], anti-inflammatory [17], antidepressant [18], and other pharmacological [19–21] capabilities. However, there are few reports on its role in bacteriostasis, and there are currently no studies exploring the application of SPEO as an antimicrobial agent in cotton knitting. SPEO has the potential to be used as a natural antimicrobial agent in textile cotton in the future; however, SPEO in its liquid state is unstable, volatile, and easily affected by external environmental factors such as light, temperature, and oxygen [22], thus limiting its application in the textile field.

Microencapsulation technology uses one or more polymerized film-forming materials to coat tiny particles of solids, liquids, or gases; these particles range in size from several nanometers to thousands of microns. Microencapsulation can change the state of substances, control the release of volatile substances, improve the hydrophilicity of plant essential oils, protect the release of core materials, and extend the storage time of active ingredients [23,24]. Liquid essential oil can be transformed into solid microcapsules by microencapsulation technology, which not only improves the stability of essential oil, but also expands the range of its possible applications in the textile industry. At present, microcapsules are mainly prepared by multiple condensation [25], spray drying [26], layer self-assembly [27], and microfluidics [28], among other methods. The complex condensation method is considered true microencapsulation because the core material is completely surrounded by a wall material. The complex condensation method has the advantages of mild processing conditions, less damage to the core material, and a high encapsulation rate [29].

Polysaccharide and protein are two kinds of natural water-soluble polymers that are—in addition to being nontoxic and harmless—easily biodegradable, making them the most commonly used composite wall materials in the complex condensation method. Chitosan, as a hydrophilic cationic polymer in polysaccharides, can protonate under acidic conditions and form a film of polyanions. It also has a good bacteriostatic ability and degradability [30,31]. Gelatin is a biodegradable, biocompatible, nontoxic, safe, and abundant water-soluble protein. The excellent properties of chitosan and gelatin have caused them to be widely used in the wall materials of microcapsules [32].

Cotton fabric is one of the most commonly used fabrics in the textile field [33] due to several advantages: it is soft, absorbs moisture well, and is good at retaining heat. In recent years, due to the impact of the novel coronavirus epidemic, people have begun to pay more attention to the antimicrobial and antiviral potential of textiles, and the technology of infusing textiles with antimicrobial agents has become a popular area of research [34].

Microcapsule technology is widely used in antimicrobial textiles because of its slow release and isolation properties [23], which enable the finished fabric to maintain its antimicrobial activity for a long time. The common antimicrobial functional finishing techniques include impregnation [35], fiber modification [36], and fabric coating [37]. The impregnation method is widely used in essential-oil microencapsulation technology because of its simplicity and negligible effect on the active substances.

In this study, four kinds of saffron petal essential oil (SPEO) were prepared from saffron petals, and the influence of different preparation methods on SPEO was investigated. Using SPEO as the core material and gelatin and chitosan as the wall material, saffron petal essential oil microcapsules (SPEO-Ms) were prepared via the complex condensation method. The embedding rate, particle morphology, slow-release effect, thermal stability, and infrared spectrum of the microcapsules were evaluated. In addition, SPEO-Ms were grafted onto knitted cotton by the impregnation method in order to imbue a functional textile with antimicrobial properties. The physical and mechanical properties of antimicrobial cotton were then evaluated, as was the effect of the preparation process on the antimicrobial properties of SPEO.

2. Materials and Methods

2.1. Materials

2.1.1. Reagents

Petroleum ether (AR) and n-hexane (AR) were provided by Wuxi Yasheng Chemical Co., Ltd. (Wuxi, China) and Shanghai Lingfeng Chemical Reagent Co., Ltd. (Shanghai, China), respectively. Ethanol (AR), ethyl acetate (AR), calcium chloride (AR), and sodium hydroxide (AR) were supplied by Nanjing Chemical Reagent Co., Ltd., Nanjing, China.

Gelatin (BR, 80%–95% deacetylation) and chitosan (CP, Type B) were purchased from Shanghai Sinopharm Chemical Reagent Co., Ltd. (Shanghai, China) The glacial acetic acid (AR) was produced by Shanghai Jiuyi Chemical Reagent Co., Ltd. (Shanghai, China). The Twain 80 was produced by McLean Biology Co., Ltd., Shanghai, China. Glutaraldehyde

(AR) was provided by Aladdin Shanghai, China. Waterborne polyurethane (F0402) was provided by Shenzhen Jitian Chemical Co., Ltd. The cotton fabric (PPJ21700034) was purchased from China Shenzhen Cotton Times Technology Co., Ltd. (Shenzhen, China).

2.1.2. Microorganisms and Growth Conditions

Escherichia coli (ATCC25922), *Staphylococcus aureus* (ATCC6538), and *Candida albicans* (ATCC10231) were purchased from Shanghai Luwei Biotechnology Co., Ltd. (Shanghai, China). The liquid culture medium, lysogenic broth, and potato dextrose agar were prepared by the Biological Laboratory of Nanjing Forestry University.

2.2. Pretreatment of Saffron Petals

Fresh saffron was dried naturally after the stamen or pistil was removed; it was then crushed with a grinder (MKCA6-2J, MASUKO, Tokyo, Japan), and the petals were sifted through a #10 mesh and placed in cold storage, away from any light sources.

2.3. Preparation of Saffron Petal Essential Oil (SPEO)

2.3.1. Steam Distillation

A quantity of 50.0 g of saffron petals was carefully weighed, after which steam distillation extraction was performed over the course of 8 h. The distillate was extracted using ethyl acetate three times, and then a small amount of anhydrous $CaCl_2$ was added and allowed to dry overnight. After filtration, the distillate was pressure-reduced and concentrated using a rotary evaporator (QYRE-2A, Qiyu Co., Ltd., Shanghai, China), to be used at a later time. The extraction rate of essential oil was calculated according to Equation (1).

2.3.2. Organic Solvent Extraction

Petroleum ether, n-hexane, and ethanol were measured out at 500 mL, and then 50.0 g of precision material was added to each of them. After being sealed, the mixtures were placed in the dark for 48 h. After drying the anhydrous $CaCl_2$, the filtrate was concentrated and decompressed for reserve use. The extraction quality of the essential oil was calculated according to Equation (1)

$$\text{Extraction rate of essential oil}(\%) = \frac{\text{The quality of the extracted essential oils}}{\text{The quality of the raw materials}} \times 100\% \quad (1)$$

2.4. GC–MS Chromatographic Conditions

The composition and content of the SPEO were analyzed by GC–MS (ISO, Cyber Technology, WA, USA). Gas chromatography conditions: a TG-5MS elastic quartz capillary column (0.25 mm × 30 mm; membrane thickness = 0.25 μm), a carrier gas consisting of high-purity helium (99.999%), and a carrier gas flow rate of 1.0 mL/min. No shunt injection was used; the sample size was 1 μL. Heating procedure: the initial temperature was 80 °C (maintained for 2 min) and was increased to 200 °C at a rate of 15 °C/min, before being increased to 280 °C at a rate of 20 °C/min. This constant temperature was maintained for 15 min. The inlet temperature was 250 °C.

Mass spectrum conditions: the MSD ion sources used EI sources, the ion source was at a temperature of 200 °C, the electron energy was 70 eV, and the scan range was 30 to 500 *m/z*. The components were determined by the NIST05 Mass Spectrometry Standard Library, and the relative contents of each component were calculated using the area normalization method.

2.5. Preparation of Saffron Petal Essential Oil Microcapsules (SPEO-Ms)

Saffron petal essential oil microcapsules were prepared using gelatin and chitosan as wall materials through the complex condensation method [38].

After several orthogonal tests, the following optimal process conditions were settled upon: (1) 1% chitosan solution (solution A) was prepared by dissolving 0.1 g of chitosan in 10 mL of 1% glacial acetic acid solution; (2) 1 g of gelatin was dissolved in 100 mL of deionized water and stirred by a magnetic stirrer (DF-101S, Shanghai Lichen Bangxi Instrument Technology Company, Shanghai, China) at 50 °C until the gelatin was completely dissolved; 1.1 g of SPEO and Tween 80 were added to the mixture at a ratio of 2:1, and the mixture was emulsified (GBP-USC201L, CSIC715, Hangzhou, China) at 700 W for 5 min until a homogeneous mixture (solution B) was obtained; (3) solution A was slowly added to solution B over the course of half an hour and was then again stirred at 600 rpm and 50 °C for 30 min to ensure that it was completely and evenly mixed; (4) the PH was adjusted (PHS-25, Shengke Instrument Equipment Co., Ltd., Shanghai, China) to 5.4 with a 10% sodium hydroxide solution and stirred continuously for 1 h at room temperature; (5) when the temperature of the overall solution dropped below 5 °C, 0.5 mL of 25% pentediol was slowly added for curing; (6) the microcapsule suspension was obtained by continuous stirring for 4 h; the microcapsule powder was obtained by filtering, washing, and drying. The temperature of the powder was brought to 4 °C and sealed for storage.

2.6. Determination of SPEO-M Encapsulation Efficiency

SPEO was diluted with ethanol and its maximum absorption wavelength was determined through full-wavelength scanning. The absorbance of different concentrations of SPEO was measured at the maximum absorption wavelength, and a standard curve was plotted. In total, 0.5 g of microcapsule powder was weighed precisely, dissolved in 50 mL of absolute ethanol, sonicated for 30 min, and centrifuged at a high speed for 10 min. The absorbance at the maximum absorption wavelength (441 nm) of the supernatant was measured, and the loading capacity of SPEO-Ms was calculated according to the drawn standard curve. The embedding rate was calculated by Equation (2) [39], and the experiment was repeated three times. The average value was used as the final result.

$$\text{Encapsulation effciency}(\%) = \frac{\text{Total amount of SPEO in microcapsules}}{\text{Initial total amount of SPEO}} \times 100\% \quad (2)$$

2.7. Surface Morphology of Microcapsules

The structure and morphology of the microcapsules were observed using an optical microscope (Dimension Edge, Bruker, Karlsruhe, Germany) and a scanning electron microscope (ESEM; Quanta 200, FEI, Hillsboro, OR, USA).

The microcapsule suspension was diluted and dropped on a glass slide. The cover glass was used to disperse it evenly before its structure was observed under an optical microscope. The microcapsule suspension was diluted in a predetermined proportion and dropped on the loading platform. After gold spraying, the morphology of the microcapsule was observed with an environmental scanning electron microscope.

2.8. Sustained Release Properties of Microcapsules

First, 10 g of SPEO-Ms (prepared under optimal conditions) was precisely weighed and placed in glass Petri dishes to be stored at a constant temperature of 25 °C. The samples were weighed at certain intervals and centrifuged in ethanol; the absorbance of the supernatant was measured, and the relative cumulative release rate was calculated according to Equation (3) to evaluate the sustained release performance of the microcapsules.

$$\text{Relative release rate}(\%) = 1 - \frac{\text{The oil content of the microcapsules at this time}}{\text{The oil content of the original microcapsules}} \times 100\% \quad (3)$$

2.9. Thermogravimetric Analysis

The thermal stability of the samples was measured via thermogravimetric analysis (TGA; 209 F1, Netzsch, Selb, Germany). A quantity of 8 mg of each of essential oil, gelatin,

chitosan, and CPEO-Ms was put into a TGA furnace. The temperature was increased from 30 to 700 °C at a constant rate of 20 °C/min, with nitrogen at a flow rate of 20 mL/min, acting as the protective gas.

2.10. Fourier Transform Infrared Spectroscopy

A Fourier transform infrared spectrometer (VERTEX 80 V, Bruker, Ettlingen, Germany) was used to test the essential oil, gelatin, chitosan, and SPEO-Ms.

2.11. Antimicrobial Properties

Escherichia coli (*ATCC25922*), Staphylococcus aureus (*ATCC6538*), and Candida albicans (*ATCC10231*) were used as experimental bacteria.

The antimicrobial properties of the samples were determined using an agar diffusion test. The filter paper (d = 6 mm) was immersed in the sample so that the sample was evenly distributed across the filter paper. The filter paper was placed on a medium (d = 90 mm) of a mixed bacterial suspension and agar (55 °C) and incubated for 24 h at 37 °C (48 h for fungi at 28 °C). The antimicrobial activity of the samples was determined by measuring the diameter of the antimicrobial zone.

The antimicrobial properties of the cotton fabric were tested via the flask oscillation method. The untreated cotton fabric ($P_{0g/L}$) and the antibacterial-treated cotton fabric ($P_{5g/L}$, $P_{10g/L}$, $P_{15g/L}$, $P_{20g/L}$) were cut into 5 mm × 5 mm pieces and weighed 0.75 g each, forming a single pattern. The pattern was then placed into a conical flask containing 70 mL of a liquid medium and 5 mL of the bacterial solution to be tested at a set temperature of 25 °C at a speed of 250 r/min, with an oscillation period of 18 h. After the oscillation, the bacterial solution was removed from the conical bottle and diluted; then, 1 mL of the diluted bacterial solution was absorbed and evenly smeared onto the solid medium. The coated petri dish was then placed into the constant temperature incubator at 37 °C for 48 h and measured. The inhibition rate was calculated according to Equation (4), where Y is the antimicrobial rate (%), W_0 is the concentration of viable bacteria in the flask of the control sample without antimicrobial treatment after 18 h of mixing (CFU/mL), and W_t is the concentration of viable bacteria (CFU/mL) in the flask after the sample has been mixed for 18 h with the antimicrobial treatment.

$$Y = \frac{W_0 - W_t}{W_t} \times 100\% \quad (4)$$

2.12. Preparation of Antimicrobial Cotton

The cotton knitting was soaked in distilled water with a small amount of caustic soda and stirred at 80 °C for 1.5 h. After this was completed, it was washed with clean water twice and set aside to dry. In order to prepare the finishing solution, different concentrations of SPEO-Ms (0, 5, 10, 15, 20 g/L), waterborne polyurethane (mass fraction 3%), and a certain amount of distilled water were mixed at room temperature for 30 min so that the microcapsules were evenly distributed in the system. Then, the pretreated cotton knitwear was put into microcapsule finishing solutions of different concentrations with a bath ratio of 1:30 and impregnated for 90 min at 40 °C. After dipping, they were baked at 80 °C for 3 min, then dried at room temperature and labeled $P_{0g/L}$, $P_{5g/L}$, $P_{10g/L}$, $P_{15g/L}$, and $P_{20g/L}$, respectively. To normalize the water content of the cotton, the treated cotton knitwear was set in an environment with a constant temperature and humidity level.

2.13. Physical Properties of Antimicrobial Cotton

An analytical balance (Statotious, Satori Instruments Co. Ltd., Beijing, China) was used to determine the gram weight of the cotton fabric. The cotton fabric was cut to 150 mm × 200 mm, weighed three times, and averaged to obtain the final result.

The whiteness of the cotton fabric was measured by a whiteness meter (WSB-2, Wenzhou Instrument Company, Wenzhou, China). The measurements were repeated five times for each pattern, and the average of the five measurements was used as the result.

The breathability test was conducted using a breathability tester (YG46E1-3, Suzhou Metrology Co. Ltd., Suzhou, China) in accordance with the GB/T-2009 standard, and the style specification was 100 mm × 100 mm. Each group tested three samples simultaneously, with pressure differences of 200 Pa. The average value was used after the test was completed.

A fabric moisture permeability meter (YG601H-2, Suzhou Metrology Co. Ltd., Suzhou, China) was used to test according to GB/T12704.1-2009. The temperature was set at 38 °C, the relative humidity was 50%, and the gas flow rate was 0.3–0.5 m/s. For each pattern, the average of the three tests was used as the result.

3. Results and Discussion

3.1. Characterization of SPEO

3.1.1. Effect of Different Extraction Methods on the Essential Oil of Saffron Petals

As can be seen in Table 1, the darker color of the essential oils extracted from organic solvents indicated that the pigments in saffron petals were more easily dissolved in organic solvents.

Table 1. Results of different extraction methods for saffron petals.

Method of Extraction	Time (h)	Morphology of Extracts	Extraction Rate (%)
Steam distillation	8	Pale yellow paste	0.17
Organic solvent extraction (n-hexane)	48	Tan paste	2.05
Organic solvent extraction (petroleum ether)	48	Tan paste	2.57
Organic solvent extraction (ethanol)	48	Dark brown paste	20.80

The extraction rates of SPEO also differed according to which of the four extraction methods were used; for example, the extraction rate when organic solvent extraction was used was higher than that which occurred via steam distillation. The extraction rates of different organic solvent extraction methods also differed considerably. While the extraction rates of petroleum ether and n-hexane were about the same, the extraction rate of ethanol was shown to be much higher than that of the other methods, reaching 20.80%. This is likely due to the difference in the polarity of different organic solvents, as well as the variability in the solubility of small molecules in saffron petals.

3.1.2. Analysis of Components

As can be seen in Table 2, a total of 70 components were identified by the four methods, and the components contained in the saffron flower petal extracts prepared by different methods varied greatly.

A total of 22 components were identified in the extracts prepared using steam distillation, among which the following components accounted for a relatively high portion of the overall content: n-hexadecanoic acid (25.33%), dodecanoic acid (16.96%), methyl linoleate (13.97%), linolic acid (12.12%), hexadecanoic acid, methyl ester (8.89%), and tetradecanoic acid (3.83%).

Table 2. Results of GCMS analysis of saffron petal extracts obtained by the four extraction methods.

Peak	Compound	Area (%)			
		Steam Distillation	Organic Solvent Extraction		
			n-Hexane	Petroleum Ether	Ethanol
1	2(5H)-Furanone	-	-	-	5.18
2	Methyl 6-oxoheptanoate	-	-	-	1.72
3	4H-Pyran-4-one,2,3-dihydro-3,5-dihydroxy-6-methyl-	-	-	-	24.81
4	2(3H)-Furanone, dihydro-4-hydroxy-	-	-	-	1.86
5	5-Hydroxymethylfurfural	-	-	-	5.47
6	2-Dimethylsilyloxytetradecane	-	-	-	2.38
7	Trioxsalen	-	-	-	4.64
8	Sucrose	-	-	-	1.18
9	Dodecanoic acid	16.96	-	-	8.63
10	n-Hexadecanoic acid	25.33	5.01	2.97	1.08
11	Heptadecanoic acid	-	-	-	1.18
12	12,15-Octadecadienoic acid, methyl ester	-	-	-	12.31
13	Linolic acid	12.12	0.97	3.21	2.31
14	11-n-Decyltetracosane	-	-	-	4.84
15	Octacosane	-	13.46	-	0.89
16	Phthalic acid, dodecyl octyl ester	-	-	-	3.91
17	3-Methylheptacosane	-	19.6	-	1.55
18	Octacosanol	-	4.5	1.91	16.06
19	3-Methylnonacosane	-	2.76	-	-
20	Nonanoic acid	1.01	-	-	-
21	[1,1′-Bicyclopropyl]-2-octanoic acid, 2′-hexyl-, methyl ester	0.81	-	-	-
22	Dodecanoic acid, methyl ester	0.66	-	-	-
23	Dodecanoic acid, TMS derivative	0.97	-	-	-
24	Tetradecanoic acid	3.83	-	-	-
25	Cyclopropanebutanoic acid, 2-[[2-[[2-[(2-pentylcyclopropyl)methyl]cyclopropyl]methyl	1.25	-	-	-
26	Pentadecanoic acid	0.97	-	-	-
27	Hexadecanoic acid, methyl ester	8.89	-	-	-
28	Hexadecanoic acid, 14-methyl-, methyl ester	1.74	-	-	-
29	Palmitic acid trimethylsilyl ester	2.47	-	-	-
30	α-Linolenic acid	0.70	-	-	-
31	methyl linoleate	13.97	-	-	-
32	Heptadecanoic acid, 16-methyl-, methyl ester	0.76	-	-	-
33	Icosanal	0.64	1.24	-	-
34	Nitrazepam	2.06	-	-	-
35	4,8,12,16-Tetramethylheptadecan-4-olide	1.01	1.79	-	-
36	Tetratetracontane	1.16	-	-	-
37	Tetracontane	1.12	-	-	-
38	1,2-Benzenedicarboxylic acid, isodecyl octyl ester	1.57	-	-	-
39	Cyclotetradecane	-	1.12	-	-
40	1-Hexadecene	-	1.8	-	-
41	(-)-Epicedrol	-	0.39	-	-
42	2-Methylheptacosane	-	0.91	-	-
43	1-Nonadecene	-	1.71	-	-
44	16-Hexadecanoyl hydrazide	-	0.45	-	-
45	1-Docosene	-	1.23	-	-
46	Heneicosane	-	1.04	-	-
47	Ethyl linoleate	-	0.44	-	-
48	n-Tetracosanol-1	-	1.05	-	-
49	Octacosane, 2-methyl	-	4.63	-	-
50	Docosanal	-	1.61	-	-
51	Nonacosane	-	26.51	-	-
52	Pentacosane	-	1.77	-	-
53	3-Methylpentacosane	-	1.20	-	-
54	Tetracosane, 11-decyl-	-	3.97	-	-
55	19-Heptatriacontanol	-	0.84	-	-
56	Undecane	-	-	8.29	-
57	Hexadecane	-	-	11.38	-
58	Methyl salicylate	-	-	4.85	-
59	Tetradecane, 2,6,10-trimethyl-	-	-	9.12	-
60	Dodecane, 2,6,11-trimethyl-	-	-	10.46	-
61	Tridecane	-	-	2.74	-
62	1-Octadecanesulphonyl chloride	-	-	3.99	-

Table 2. *Cont.*

Peak	Compound	Area (%)			
		Steam Distillation	Organic Solvent Extraction		
			n-Hexane	Petroleum Ether	Ethanol
63	Octadecane, 6-methyl-	-	-	2.20	-
64	Tetradecane	-	-	14.71	-
65	Hexadecane, 2,6,11,15-tetramethyl-	-	-	8.93	-
66	Pentadecane, 2,6,10-trimethyl-	-	-	2.40	-
67	Eicosane, 2-methyl-	-	-	6.44	-
68	Docosane	-	-	1.88	-
69	Heptacosane	-	-	2.96	-
70	Octadecane, 1-chloro-	-	-	1.56	-

"-" indicates absence of the compound.

A total of 25 components were identified in the extract prepared via organic solvent extraction (n-hexane), and the components accounting for a relatively high portion of the overall content as revealed by this method were nonacosane (26.51%), 3-methylheptacosane (19.6%), octacosane (13.46%), n-hexadecanoic acid (5.01%), octacosane, 2-methyl (4.63), octacosanol (4.5%), and tetracosane, 11-decyl- (3.97%).

A total of 18 components were identified in the extracts prepared via organic solvent extraction (petroleum ether), among which the following components accounted for a relatively high portion of the overall content: tetradecane (14.71%), hexadecane (11.38%), dodecane, 2,6,11-trimethyl- (10.46%), tetradecane, 2,6,10-trimethyl- (9.12%), hexadecane,2,6,11,15-tetramethyl- (8.93%), undecane (8.29%), eicosane, 2-methyl- (6.44%), methyl salicylate (4.85%), and 1-octadecanesulphonyl chloride (3.99%).

A total of 18 components were identified in the extracts prepared via organic solvent extraction (ethanol), among which the following components accounted for a relatively high portion of the overall content: 4H-pyran-4-one,2,3-dihydro-3,5-dihydroxy-6-methyl- (24.81%), octacosanol (16.06%), 12,15-octadecadienoic acid, methyl ester (12.31%), dodecanoic acid (8.63%), 5-hydroxymethylfurfural (5.47%), 2(5H)-furanone (5.18%), 11-n-decyltetracosane (4.84%), trioxsalen (4.64%), and phthalic acid, dodecyl octyl ester (3.91%).

By comparison, n-hexadecanoic acid and linoleic acid were present in the extracts produced by all four extraction methods. Studies have shown that n-hexadecanoic acid has antioxidant and antimicrobial abilities [40]. The higher proportions of 4H-pyran-4-one,2,3-dihydro-3,5-dihydroxy-6-methyl- (DDMP), octacosanol, dodecanoic acid, and 2(5H)-furanone in ethanol extract from saffron petals suggest a strong biological activity. Studies have shown that DDMP is a strong antioxidant [41] and octacosanol can treat and prevent various metabolic and cardiovascular diseases [42], while dodecanoic acid and 2(5H)-furanone have antimicrobial and antifungal properties [43,44]. It may be that the synergistic action of these active substances causes the ethanol extract of saffron petals to display its strong inhibitory effect on *Escherichia coli*, *Staphylococcus aureus*, and *Candida albicans*. This also reveals the potential application of the ethanol extract of saffron petals as a new, natural antimicrobial agent.

3.1.3. Antimicrobial Capacity of SPEO

Measuring the antimicrobial zone diameter is one of the effective methods used to judge the antimicrobial performance of extracts.

From Figures 1–3 and Table 3, it can be seen that the antimicrobial activity of SPEO prepared by different extraction methods was significantly different. SPEO extracted with n-hexane had no significant inhibitory effect on *S. aureus*, while SPEO extracted with steam distillation and petroleum ether only had a significant inhibitory effect on *S. aureus*. However, the SPEO extracted from the organic solvent (ethanol) had obvious inhibitory effects on *Escherichia coli*, *Staphylococcus aureus*, and especially on *Candida albicans*. As shown in Table 3, the diameter of the antimicrobial zone in this instance reached 16.1 mm. From

this, one may conclude that differences in the content of SPEO components extracted by different extraction methods led to differences in antimicrobial activity.

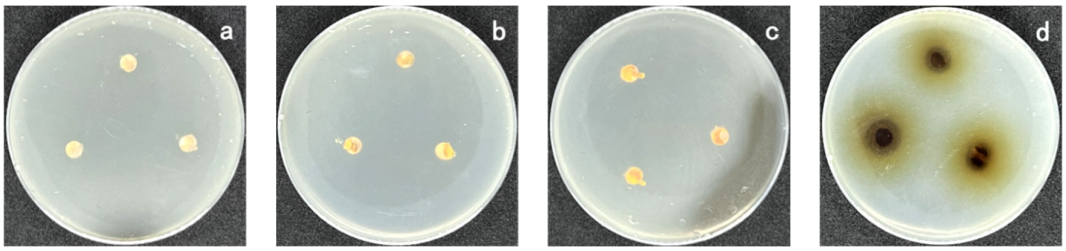

Figure 1. Inhibition of steam distillation extract (**a**), n-hexane extract (**b**), petroleum ether extract (**c**), and ethanol extract (**d**) on *Escherichia coli*.

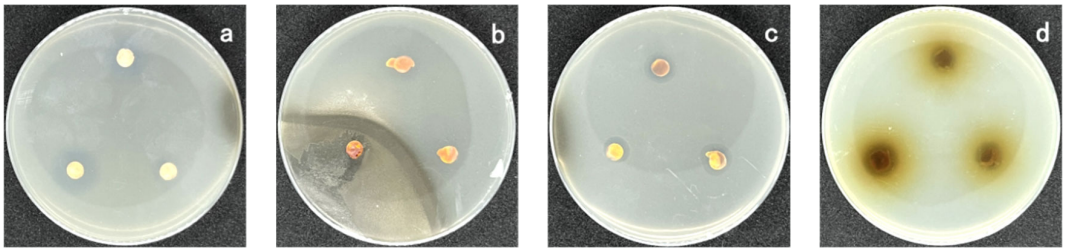

Figure 2. Inhibitory effects of steam distillation extract (**a**), n-hexane extract (**b**), petroleum ether extract (**c**), and ethanol extract (**d**) on *Staphylococcus aureus*.

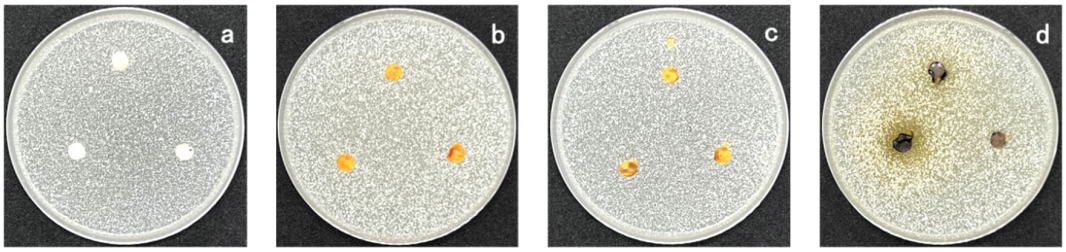

Figure 3. Inhibitory effects of steam distillation extract (**a**), n-hexane extract (**b**), petroleum ether extract (**c**), and ethanol extract (**d**) on *Candida albicans*.

Table 3. Diameter of antimicrobial zone of different extracts against *E. coli*, *S. aureus*, and *C. albicans*.

Method of Extraction	*E. coli* (mm)	*S. aureus* (mm)	*C. albicans* (mm)
Steam distillation	-	12.1 ± 0.7	-
Organic solvent extraction/(n-hexane)	-	-	-
Organic solvent extraction (petroleum ether)	-	11.2 ± 0.6	-
Organic solvent extraction (ethanol)	11.2 ± 0.4	12.4 ± 0.9	16.1 ± 1.1

"-" indicates no obvious bacteriostatic performance (diameter of the bacteriostatic zone < 6 mm).

3.2. Characterization of SPEO-Ms

3.2.1. UV Standard Curve for SPEO

The absorbance of different SPEO concentrations was measured with an ultraviolet spectrophotometer (Tu-1900, AOE Instruments, Shanghai, China) at 441 nm. The resulting standard curve ($y = 2.7415x + 0.0088$, $R^2 = 0.9919$) is shown in Figure 4. The results show that the SPEO concentration was linearly correlated with the peak area.

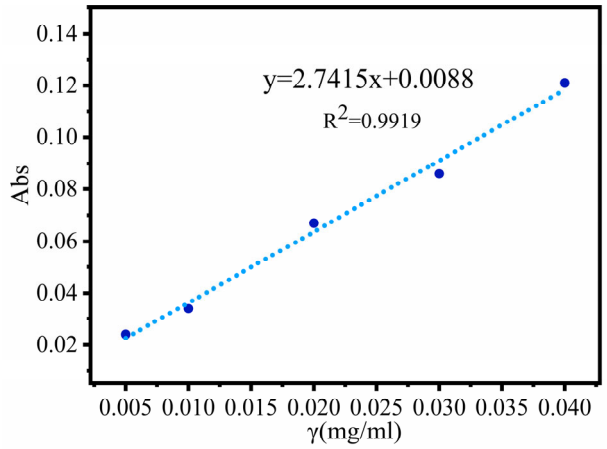

Figure 4. UV standard curve for SPEO.

3.2.2. Microcapsule Structure Analysis

The surface structure of the SPEO-Ms is shown in Figure 5. The microcapsule structure was spherical and maintained a uniform size, and the surface was smooth, without obvious depressions or notches. This is because glutaraldehyde can react with nitrogen atoms on the amide and amine groups of gelatin and chitosan to form covalent bonds, allowing the essential oil to be wrapped in them [45]. However, under the condition of rapid drying, it can be seen from the figure that an adhesion between microcapsules takes place.

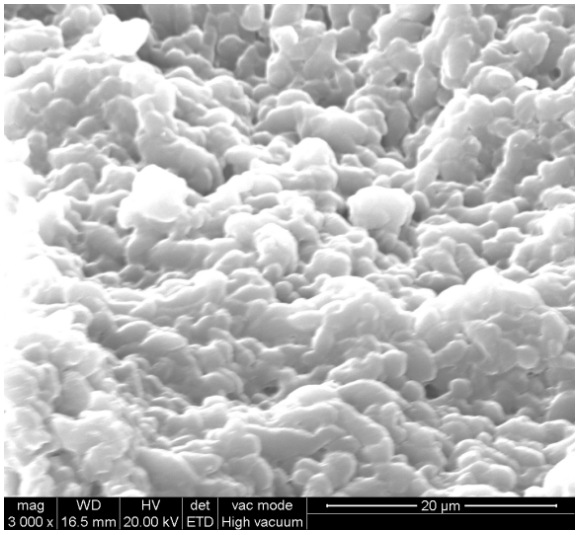

Figure 5. ESEM images of SPEO-Ms at magnification of 3000×.

3.2.3. Morphology

Figure 6 shows the macroscopic and microscopic morphology of the microcapsule suspension. Figure 6a shows that the microcapsule suspension was stratified: the lower layer consisted of precipitated microcapsule particles, and there was no yellow oil layer in the upper layer, which indicated that the SPEO was successfully coated. Figure 6b shows a microscopic image of SPEO-Ms. In this image, the microcapsules were well-dispersed. Based on the microcapsules with larger particle sizes, it was obvious that they had a multicore structure with SPEO wrapped inside of it. This structure allowed the microcapsule to better control the release of the SPEO core.

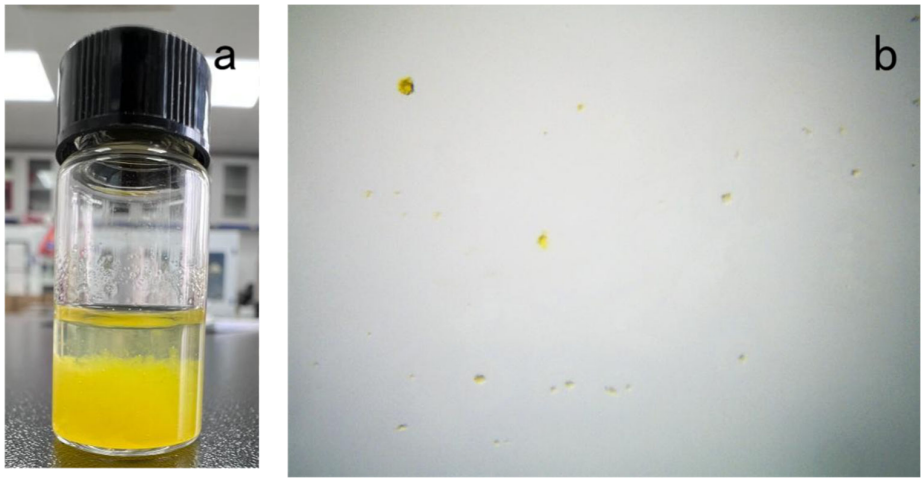

Figure 6. The macroscopic (**a**) and microscopic (**b**) morphology of the microcapsule suspension.

3.2.4. Sustained-Release Effect

Figure 7 shows that SPEO-Ms exhibited a sustained release behavior that tended to be flat and was mainly divided into a fast-release phase and a stable-release velocity phase. During the first stage (0–8 d), the release rate of the microcapsule core material was faster, which was due to the high oil content of the newly prepared SPEO-Ms and the large difference in the concentration of essential oil inside and outside the microcapsule. In the second stage (8–15 d), the release of SPEO tended to be flat mainly because the release rate of SPEO decreased as the release time increased; meanwhile, the difference in SPEO concentrations between microcapsules decreased, along with those inside the microcapsules. After 10 days, the retained microcapsule core material still accounted for 54% of the initial microcapsule core material, indicating that microcapsule technology was capable of delaying the release of essential oils. Compared with the microcapsules prepared by other preparation methods, they showed the characteristics of a rapid release in the early stage and stable release in the late stage [46]. However, the release curve in this study was relatively flat, which was probably caused by the difference in wall materials and preparation methods [47].

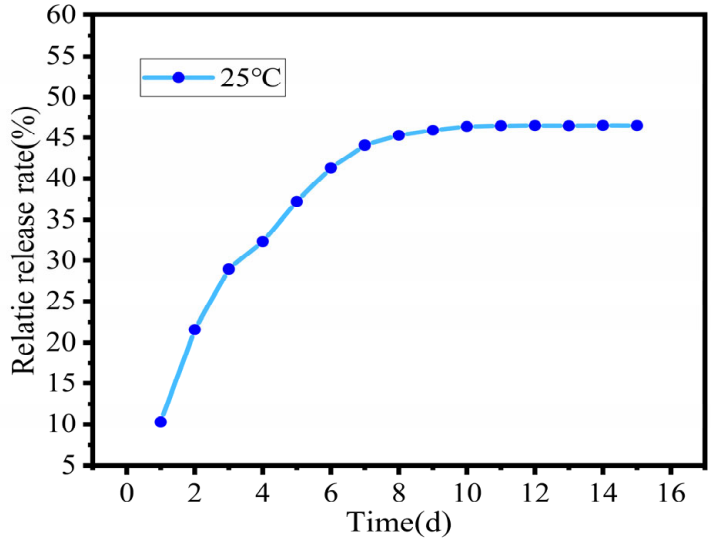

Figure 7. Sustained-release performance of SPEO-Ms.

3.2.5. Thermal Stability

The thermogravimetric analysis is one of the important indexes used to evaluate the thermal stability of materials. As can be seen in Figure 8, SPEO was very sensitive to heat,

and its mass decreased rapidly between 35 °C and 100 °C, indicative of SPEO volatility. At this temperature, the mass of SPEO-Ms hardly changed, because the microencapsulated SPEO was coated with complex agglomerates formed by gelatin and chitosan. As these had a good thermal stability, they were able to confer this property to SPEO-Ms as well. When combined with DTG (see Figure 8b), the decomposition process of microcapsules mainly occurred between 210 °C and 435 °C. This was because electrostatic attraction had broken the covalent bond between the gelatin and chitosan, destroying the original complex condensates [48]. In the final stage (435–700 °C), the core material was completely released, and the carbonization of the organic matter that followed the decomposition of the wall material accounted for the slow reduction of the weight loss rate [49].

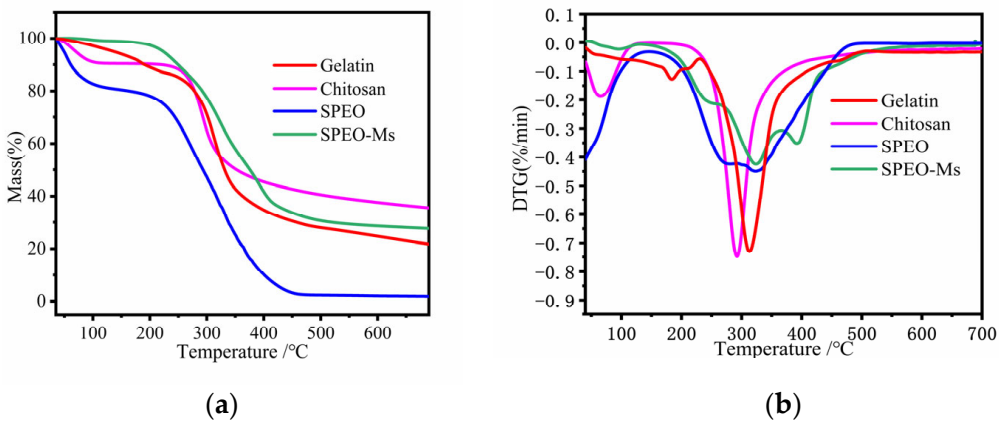

Figure 8. TGA (**a**) and DTG (**b**) curves for gelatin, chitosan, SPEO and SPEO microcapsules.

3.2.6. FTIR Analysis

Figure 9 shows the FTIR spectra of gelatin, chitosan, SPEO, and SPEO-Ms. The characteristic peaks of gelatin were located at 3432 cm^{-1}, 2974 cm^{-1}, 1637 cm^{-1}, and 1237 cm^{-1}, corresponding to amino N–H stretching vibrations, alkyl C–H stretching vibrations, amide carbonyl C=O stretching vibrations, and C–N stretching vibrations of atoms in the amide bond, respectively.

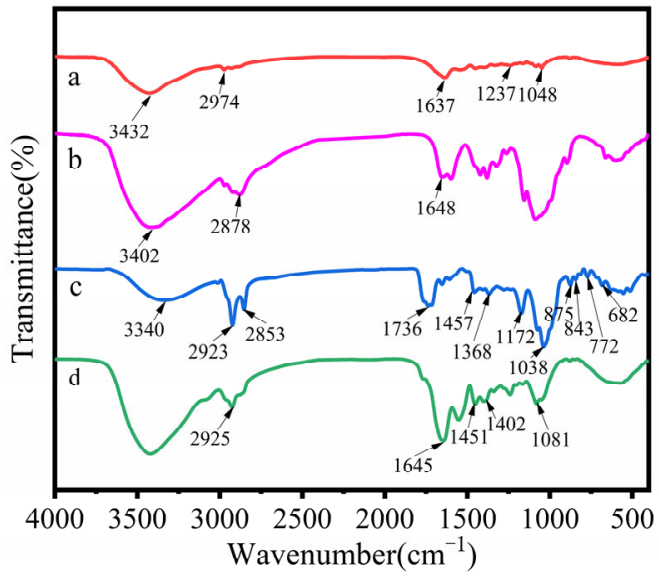

Figure 9. FTIR spectra: a = gelatin; b = chitosan; c = SPEO; d = SPEO microcapsules.

The characteristic peaks of chitosan could be attributed to -NH_2 and -OH stretching vibrations (3402 cm^{-1}), C–H stretching vibrations (2878 cm^{-1}), and characteristic amide absorption (1648 cm^{-1}).

The hydroxyl group, carboxylic acid, and amine in gelatin can form hydrogen bonds with the hydroxyl group and ammonium group in chitosan, thereby encapsulating SPEO [50].

The wave number of the characteristic peak of SPEO was 3340 cm^{-1}; the wide peak corresponded to the hydroxy-OH stretching vibration peak; the 2923 and 2853 cm^{-1} peaks belonged to the C–H antisymmetric stretching vibration peak and symmetric stretching vibration peak in the methylene group and methyl group, respectively; the 1736 cm^{-1} peak belonged to the carbonyl C=O stretching vibration peak; the 1457 cm^{-1} peak belonged to the C=C skeleton vibration in the benzene ring. The peak at 1368 cm^{-1} was the C–H bending vibration peak in the saturated hydrocarbon group; the peaks at 1172 cm^{-1} and 1038 cm^{-1} corresponded to the C–O stretching vibration peak; and the peaks at 875, 843, 772, and 682 cm^{-1} corresponded to the oscillating vibration in the C–H plane on the benzene ring.

The FTIR spectrum of SPEO-Ms contained the characteristic peak of SPEO, and the corresponding absorption peaks of the benzene ring and carbonyl group were significantly weakened, confirming that SPEO was successfully encapsulated by the wall material.

3.2.7. Antimicrobial Activity

The bacteriostatic effect of SPEO-Ms on *Escherichia coli*, *Staphylococcus aureus*, and *Candida albicans* is shown in Figure 10. It can be seen that SPEO-Ms prepared after being embedded with SPEO maintained excellent antimicrobial activity. The average diameters of the antimicrobial zones were 11.2, 11.5, and 13.8 mm, respectively. Compared with the SPEO-Ms analyzed before embedding (Table 3), the size of the bacteriostatic zone was slightly decreased, which may have been caused by a decrease in essential oil concentration after embedding. However, the prepared SPEO-Ms also possessed a slow-release capability, allowing them to maintain their antimicrobial ability for a longer period of time.

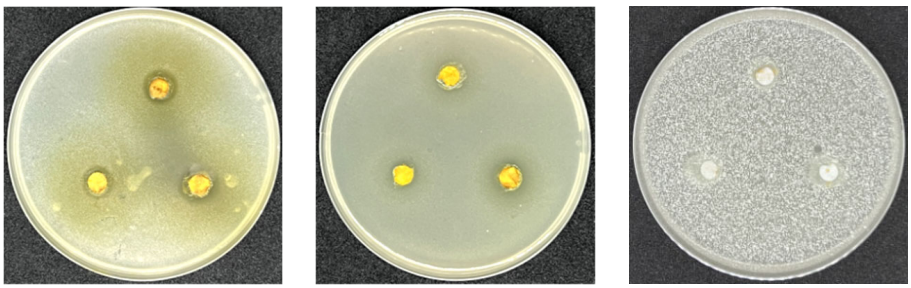

Figure 10. Antimicrobial effect of SPEO-Ms on *E. coli*, *S. aureus*, and *C. albicans*.

3.3. Characterization of Antimicrobial Cotton Knitwear

3.3.1. Surface Morphology

Figure 11 shows cotton fabric containing different concentrations of microcapsules. It can be seen from Figure 11f that the SPEO-Ms successfully adhered to the cotton fabric, and the microcapsule morphology still maintained its spherical shape without ruptures or depressions. As the concentration of microcapsules increased, the microcapsules agglomerated on the fiber surface. When the concentration of microcapsules reached 20 g/L, an extreme agglomeration of microcapsules occurred, so that a large number of microcapsules did not adhere to the fiber surface uniformly (Figure 11e).

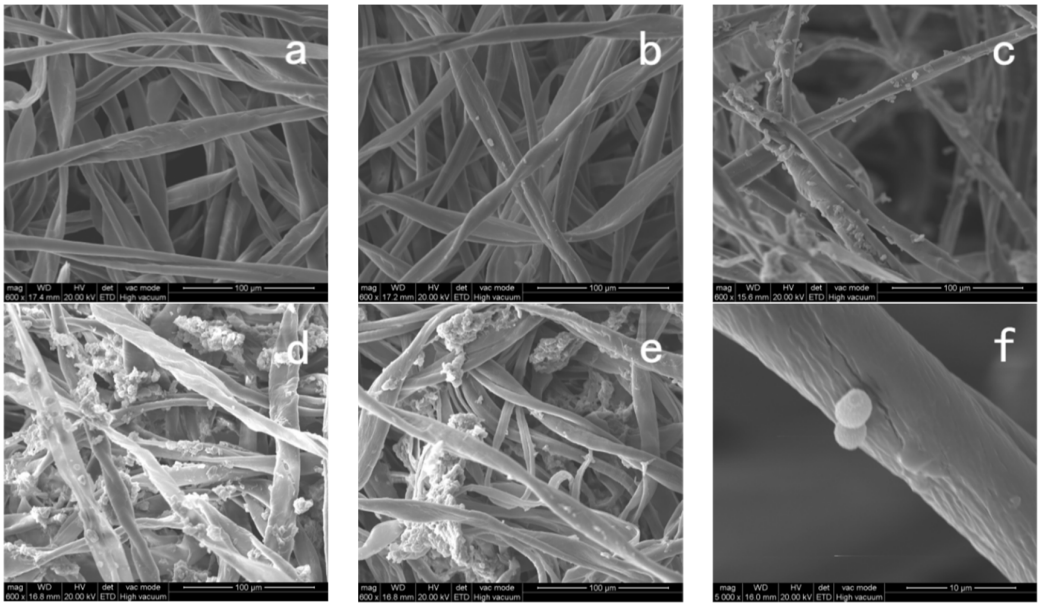

Figure 11. Sem images of (**a**) $P_{0g/L}$, (**b**) $P_{5g/L}$, (**c**) $P_{10g/L}$, (**d**) $P_{15g/L}$, (**e**) $P_{20g/L}$ at 600× magnification and (**f**) $P_{5g/L}$ at magnification of 5000×.

3.3.2. Physical Properties

Table 4 lists the results for gram weight, whiteness, and permeability of raw cotton fabric and antimicrobial cotton containing different concentrations of microcapsules. The weight and whiteness of the original cotton fabric were 1.50 g and 82.1%, respectively. With the increase of microcapsule concentration, the gram weight of the antimicrobial cotton initially increased rapidly and then slowly, while the whiteness decreased rapidly and then slowly, which confirmed that the microcapsule successfully adhered to the surface of the cotton fiber. When the microcapsule concentration reached 15 gL^{-1}, the microcapsule concentration on the cotton fabric was close to saturation, at which point the gram weight and whiteness of the cotton fabric changed slowly as the microcapsule concentration increased. This was likely due to the agglomeration of microcapsules that could not effectively adhere to the fiber surface as the concentration of microcapsules increased.

Table 4. Weight, whiteness, MAP, and WVP of untreated cotton and antimicrobial cotton.

Sample	Grammage (g)	Whiteness (%)	MAP (mm s^{-1})	WVP (g m^{-2} day^{-1})
$P_{0\,g/L}$	1.50 ± 0.13	82.11 ± 1.50	1658 ± 12.33	4233.02 ± 16.33
$P_{5\,g/L}$	1.68 ± 0.11	61.30 ± 2.23	1568 ± 14.20	4165.42 ± 17.52
$P_{10\,g/L}$	1.82 ± 0.12	55.10 ± 2.89	1436 ± 11.28	4112.65 ± 16.82
$P_{15\,g/L}$	1.98 ± 0.08	45.33 ± 3.33	1262 ± 15.60	3998.30 ± 15.21
$P_{20\,g/L}$	2.08 ± 0.15	44.18 ± 5.50	1366 ± 18.63	4031.71 ± 8.62

The air permeability method (MAP) describes the property of air passing through the pores of a fabric from the high-pressure side to the low-pressure side. As shown in Table 4, the air permeability of the cotton fabric without antimicrobial treatment was 1658 mm s^{-1}; the degree of air permeability initially decreased before rising with the increase in microcapsule concentration. When the microcapsule concentration reached 15 gL^{-1}, the air permeability reached 1262 mm s^{-1}. This was due to (1) the use of a binder in the preparation of the antimicrobial cotton, which, after drying, pulled the bond between the fibers closer; and (2) microcapsules filling the pores between the fibers, resulting in a decrease in air permeability. However, when the microcapsule concentration was too

high, a poor bonding of the interface between the two phases occurred due to the clumped microcapsules, promoting the diffusion of gas molecules between the fibers and increasing the air permeability.

Water vapor permeability (WVP) refers to the difference in water vapor pressure between the two sides of the material based on the specified temperature and relative humidity, as well as the amount of water vapor transmitted by the material of 1 square meter within 24 h [51]. As can be seen from Table 4, an increase in microcapsule concentration also caused WVP to initially decrease, but then increase. This trend may be attributable to the same factors that were observed to influence MAP; namely, that the adhesive and microcapsules caused the fibers to become more tightly bonded, reducing the number of pores. When the microcapsule concentration was too high, the free space volume in the system decreased due to the agglomeration of microcapsules, so the WVP also increased.

3.3.3. Antimicrobial Activity

The oscillating flask method is an effective method for performing a quantitative analysis on the antimicrobial properties of cotton fabrics. Figures 12–14 show the inhibitory effects of antimicrobial cotton containing different concentrations of SPEO-Ms on *Escherichia coli*, *Staphylococcus aureus*, and *Candida albicans*. When Figures 12–14 are considered along with Table 5, it becomes clear that the treated cotton fabric had a significant inhibitory effect on bacteria and fungi. With the increase in microcapsule concentration, the antimicrobial rate of the cotton fabric also increased. When the concentration of microcapsules reached 15 g/L, the antimicrobial rates of the cotton fabrics against *Escherichia coli*, *Staphylococcus aureus*, and *Candida albicans* reached 88.89%, 90.20%, and 96.13%, respectively. When the microcapsule concentration was increased, the antimicrobial effect remained almost the same. This suggested that when the microcapsule concentration reached 15 g/L, the microcapsule content on the cotton fabric reached its saturation state.

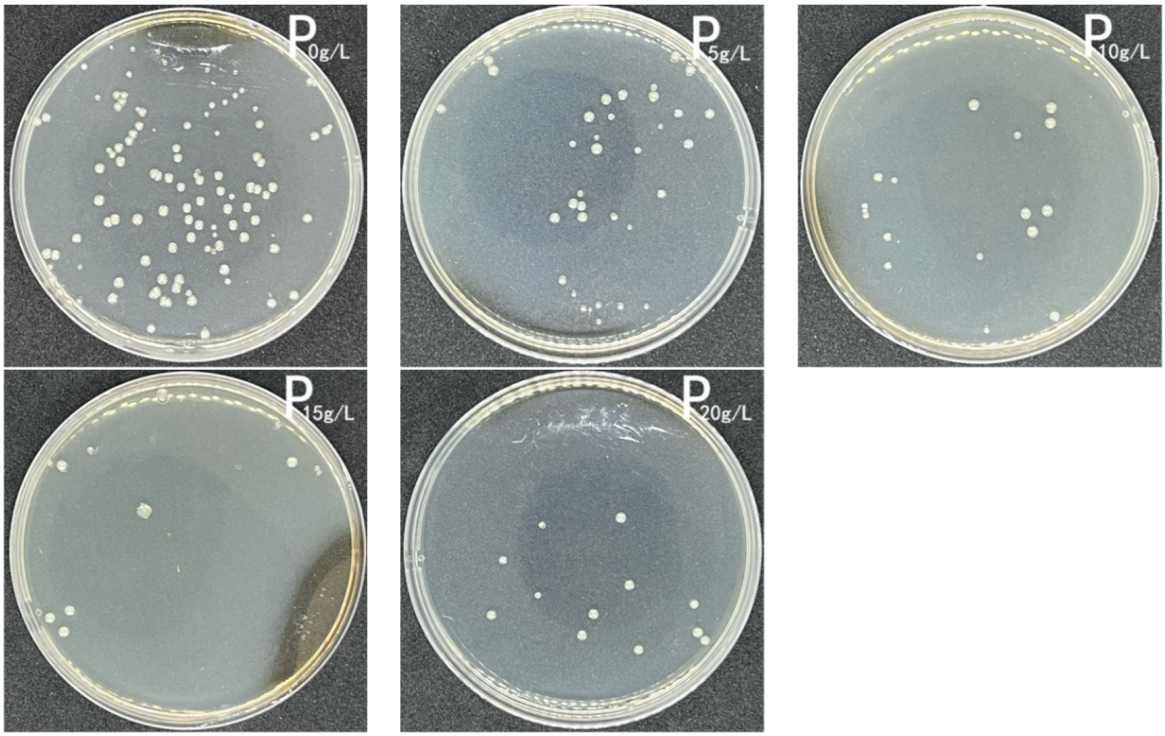

Figure 12. Inhibition of *E. coli* by untreated cotton and antimicrobial cotton.

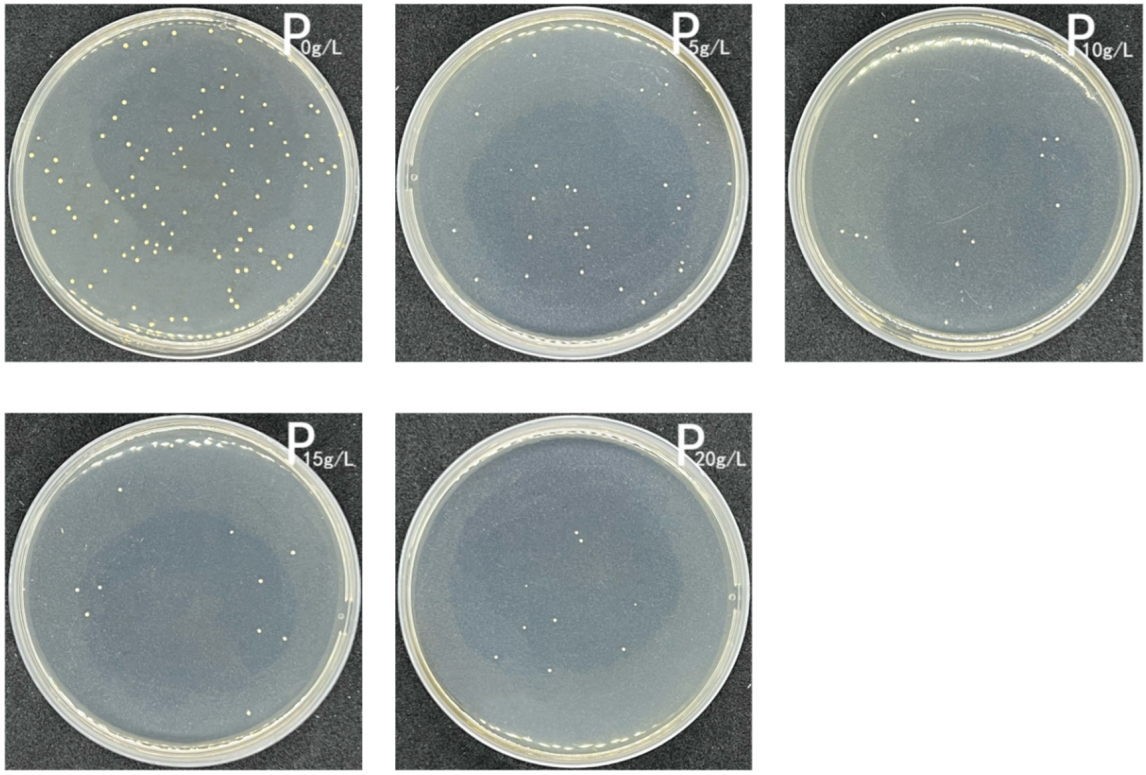

Figure 13. Inhibition of *S. aureus* by untreated cotton and antimicrobial cotton.

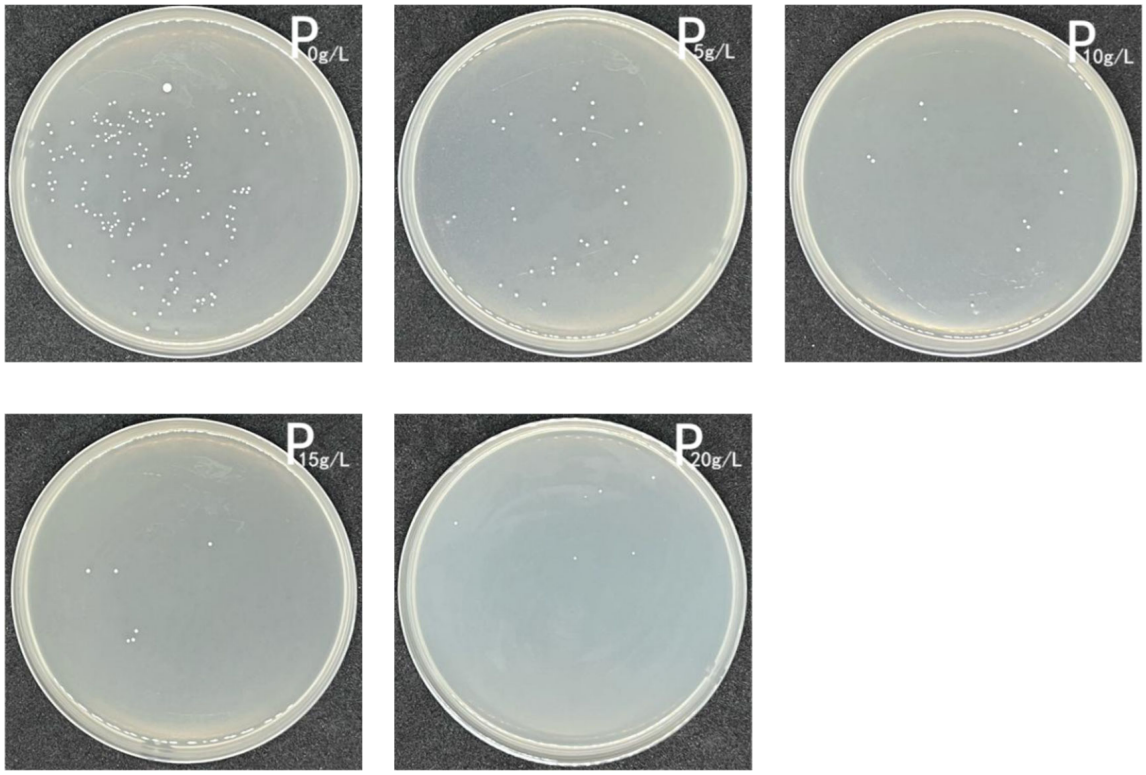

Figure 14. Inhibition of *C. albicans* by untreated cotton and antimicrobial cotton.

Table 5. Inhibition rates of untreated cotton and antimicrobial cotton against *E. coli*, *S. aureus*, and *C. albicans*.

Sample	*E. coli*		*S. aureus*		*C. albicans*	
	Colony Counting (CFU mL^{-1} 10^{-6})	Inhibition Rate (%)	Colony Counting (CFU mL^{-1} 10^{-6})	Inhibition Rate (%)	Colony Counting (CFU mL^{-1} 10^{-6})	Inhibition Rate (%)
$P_{0g/L}$	117	-	102	-	155	-
$P_{5g/L}$	35	70.09	30	70.59	34	76.06
$P_{10g/L}$	18	84.62	14	86.27	13	91.61
$P_{15g/L}$	12	88.89	10	90.20	6	96.13
$P_{20g/L}$	12	88.89	9	91.18	6	96.13

4. Conclusions

SPEO extracted via an organic solvent extraction method had a higher extraction rate and better bacteriostatic ability than that extracted by other methods. The encapsulation rate of SPEO-Ms was 65.52% when the composite condensation method was used, wherein gelatin and chitosan served as the wall materials. The strong bonding between the two wall materials was confirmed by ESEM and FTIR. TGA and sustained-release experiments showed that the synthesized microcapsules had a good stability and the ability to slow the release of core material. The microcapsules were successfully adhered to cotton fibers utilizing the dipping method. The addition of microcapsules could reduce the whiteness, air permeability, and moisture permeability of cotton fabric. When the concentration of microcapsules reached 15 g/L, the concentration of microcapsules that adhered to the cotton fiber reached a saturation point. Inhibition tests showed that although the inhibitory capacity of SPEO decreased due several factors, it maintained its inhibition capacity against *E. coli*, *Staphylococcus aureus*, and *Candida albicans*. These results show that SPEO-Ms can be used as a natural antimicrobial agent in the preparation of antimicrobial cotton fabric.

Author Contributions: Conceptualization, S.L. and L.S.; Investigation, S.L.; writing—original draft, S.L.; resources, Q.C.; supervision, M.W.; data curation, M.L., S.L., X.S. and W.C. All authors have read and agreed to the published version of the manuscript.

Funding: This research received no external funding.

Institutional Review Board Statement: Not applicable.

Informed Consent Statement: Not applicable.

Data Availability Statement: The data presented in this study are available in the article.

Conflicts of Interest: The authors declare no conflict of interest.

References

1. Pavlić, B.; Teslić, N.; Zengin, G.; Đurović, S.; Rakić, D.; Cvetanović, A.; Gunes, A.K.; Zeković, Z. Antioxidant and Enzyme-Inhibitory Activity of Peppermint Extracts and Essential Oils Obtained by Conventional and Emerging Extraction Techniques. *Food Chem.* **2021**, *338*, 127724. [CrossRef] [PubMed]
2. Aumeeruddy-Elalfi, Z.; Lall, N.; Fibrich, B.; Blom van Staden, A.; Hosenally, M.; Mahomoodally, M.F. Selected essential oils inhibit key physiological enzymes and possess intracellular and extracellular antimelanogenic properties in vitro. *J. Food Drug Anal.* **2018**, *26*, 232–243. [CrossRef]
3. Fierascu, R.C.; Fierascu, I.C.; Dinu-Pirvu, C.E.; Fierascu, I.; Paunescu, A. The Application of Essential Oils as a Next-Generation of Pesticides: Recent Developments and Future Perspectives. *Z. Für Nat. C* **2020**, *75*, 183–204. [CrossRef] [PubMed]
4. Esmaeili, Y.; Paidari, S.; Baghbaderani, S.A.; Nateghi, L.; Al-Hassan, A.A.; Ariffin, F. Essential Oils as Natural Antimicrobial Agents in Postharvest Treatments of Fruits and Vegetables: A Review. *Food Meas.* **2022**, *16*, 507–522. [CrossRef]
5. Semeniuc, C.; Socaciu, M.-I.; Socaci, S.; Mureșan, V.; Fogarasi, M.; Rotar, A. Chemometric Comparison and Classification of Some Essential Oils Extracted from Plants Belonging to Apiaceae and Lamiaceae Families Based on Their Chemical Composition and Biological Activities. *Molecules* **2018**, *23*, 2261. [CrossRef]
6. Ozdemir, N.; Bayrak, A.; Tat, T.; Yanık, Z.N.; Altay, F.; Halkman, A.K. Fabrication and Characterization of Basil Essential Oil Microcapsule-Enriched Mayonnaise and Its Antimicrobial Properties against Escherichia Coli and Salmonella Typhimurium. *Food Chem.* **2021**, *359*, 129940. [CrossRef]

7. Kord Heydari, M.; Assadpour, E.; Jafari, S.M.; Javadian, H. Encapsulation of Rose Essential Oil Using Whey Protein Concentrate-Pectin Nanocomplexes: Optimization of the Effective Parameters. *Food Chem.* **2021**, *356*, 129731. [CrossRef] [PubMed]
8. Chen, X.; Chen, W.; Lu, X.; Mao, Y.; Luo, X.; Liu, G.; Zhu, L.; Zhang, Y. Effect of Chitosan Coating Incorporated with Oregano or Cinnamon Essential Oil on the Bacterial Diversity and Shelf Life of Roast Duck in Modified Atmosphere Packaging. *Food Res. Int.* **2021**, *147*, 110491. [CrossRef] [PubMed]
9. Al-Moghazy, M.; El-sayed, H.S.; Salama, H.H.; Nada, A.A. Edible Packaging Coating of Encapsulated Thyme Essential Oil in Liposomal Chitosan Emulsions to Improve the Shelf Life of Karish Cheese. *Food Biosci.* **2021**, *43*, 101230. [CrossRef]
10. Basak, S.; Singh, J.K.; Morri, S.; Shetty, P.H. Assessment and Modelling the Antibacterial Efficacy of Vapours of Cassia and Clove Essential Oils against Pathogens Causing Foodborne Illness. *LWT* **2021**, *150*, 112076. [CrossRef]
11. Chen, Z.; Gu, J.; Lin, S.; Xu, Z.; Xu, H.; Zhao, J.; Feng, P.; Tao, Y.; Chen, S.; Wang, P. Saffron Essential Oil Ameliorates CUMS-Induced Depression-like Behavior in Mice via the MAPK-CREB1-BDNF Signaling Pathway. *J. Ethnopharmacol.* **2023**, *300*, 115719. [CrossRef] [PubMed]
12. Aboutorab, M.; Ahari, H.; Allahyaribeik, S.; Yousefi, S.; Motalebi, A. Nano-Emulsion of Saffron Essential Oil by Spontaneous Emulsification and Ultrasonic Homogenization Extend the Shelf Life of Shrimp (Crocus Sativus L.). *J. Food Process. Preserv.* **2021**, *45*, e15224. [CrossRef]
13. Rajabi, H.; Jafari, S.M.; Rajabzadeh, G.; Sarfarazi, M.; Sedaghati, S. Chitosan-Gum Arabic Complex Nanocarriers for Encapsulation of Saffron Bioactive Components. *Colloids Surf. A Physicochem. Eng. Asp.* **2019**, *578*, 123644. [CrossRef]
14. Kanakis, C.D.; Daferera, D.J.; Tarantilis, P.A.; Polissiou, M.G. Qualitative Determination of Volatile Compounds and Quantitative Evaluation of Safranal and 4-Hydroxy-2,6,6-Trimethyl-1-Cyclohexene-1-Carboxaldehyde (HTCC) in Greek Saffron. *J. Agric. Food Chem.* **2004**, *52*, 4515–4521. [CrossRef] [PubMed]
15. Serrano-Díaz, J.; Sánchez, A.M.; Martínez-Tomé, M.; Winterhalter, P.; Alonso, G.L. Flavonoid Determination in the Quality Control of Floral Bioresidues from *Crocus Sativus* L. *J. Agric. Food Chem.* **2014**, *62*, 3125–3133. [CrossRef]
16. Termentzi, A.; Kokkalou, E. LC-DAD-MS (ESI+) Analysis and Antioxidant Capacity of Crocus Sativus Petal Extracts. *Planta Med.* **2008**, *74*, 573–581. [CrossRef]
17. Hosseinzadeh, H.; Younesi, H.M. Antinociceptive and Anti-Inflammatory Effects of Crocus Sativus L. Stigma and Petal Extracts in Mice. *BMC Pharmacol.* **2002**, *2*, 7. [CrossRef]
18. Akhondzadeh Basti, A.; Moshiri, E.; Noorbala, A.-A.; Jamshidi, A.-H.; Abbasi, S.H.; Akhondzadeh, S. Comparison of Petal of Crocus Sativus L. and Fluoxetine in the Treatment of Depressed Outpatients: A Pilot Double-Blind Randomized Trial. *Prog. Neuro-Psychopharmacol. Biol. Psychiatry* **2007**, *31*, 439–442. [CrossRef]
19. Fatehi, M.; Rashidabady, T.; Fatehi-Hassanabad, Z. Effects of Crocus Sativus Petals' Extract on Rat Blood Pressure and on Responses Induced by Electrical Field Stimulation in the Rat Isolated Vas Deferens and Guinea-Pig Ileum. *J. Ethnopharmacol.* **2003**, *84*, 199–203. [CrossRef]
20. Azarmehr, N.; Afshar, P.; Moradi, M.; Sadeghi, H.; Sadeghi, H.; Alipoor, B.; Khalvati, B.; Barmoudeh, Z.; Abbaszadeh-Goudarzi, K.; Doustimotlagh, A.H. Hepatoprotective Effect of Crocus Sativus (Saffron) Petals Extract against Acetaminophen Toxicity in Male Wistar Rats. *Heliyon* **2019**, *5*, e02072. [CrossRef]
21. Zheng, C.-J.; Li, L.; Ma, W.-H.; Han, T.; Qin, L.-P. Chemical Constituents and Bioactivities of the Liposoluble Fraction from Different Medicinal Parts of Crocus Sativus. *Pharm. Biol.* **2011**, *49*, 756–763. [CrossRef] [PubMed]
22. Sutaphanit, P.; Chitprasert, P. Optimisation of Microencapsulation of Holy Basil Essential Oil in Gelatin by Response Surface Methodology. *Food Chem.* **2014**, *150*, 313–320. [CrossRef] [PubMed]
23. Jyothi, N.V.N.; Prasanna, P.M.; Sakarkar, S.N.; Prabha, K.S.; Ramaiah, P.S.; Srawan, G.Y. Microencapsulation Techniques, Factors Influencing Encapsulation Efficiency. *J. Microencapsul.* **2010**, *27*, 187–197. [CrossRef] [PubMed]
24. Ju, J.; Xie, Y.; Guo, Y.; Cheng, Y.; Qian, H.; Yao, W. Application of Starch Microcapsules Containing Essential Oil in Food Preservation. *Crit. Rev. Food Sci. Nutr.* **2020**, *60*, 2825–2836. [CrossRef]
25. Ban, Z.; Zhang, J.; Li, L.; Luo, Z.; Wang, Y.; Yuan, Q.; Zhou, B.; Liu, H. Ginger Essential Oil-Based Microencapsulation as an Efficient Delivery System for the Improvement of Jujube (*Ziziphus Jujuba* Mill.) Fruit Quality. *Food Chem.* **2020**, *306*, 125628. [CrossRef]
26. Parthasarathi, S.; Anandharamakrishnan, C. Enhancement of Oral Bioavailability of Vitamin E by Spray-Freeze Drying of Whey Protein Microcapsules. *Food Bioprod. Process.* **2016**, *100*, 469–476. [CrossRef]
27. Wang, J.; Oussama Khelissa, S.; Chihib, N.-E.; Dumas, E.; Gharsallaoui, A. Effect of Drying and Interfacial Membrane Composition on the Antimicrobial Activity of Emulsified Citral. *Food Chem.* **2019**, *298*, 125079. [CrossRef]
28. Du, Y.; Mo, L.; Wang, X.; Wang, H.; Ge, X.; Qiu, T. Preparation of Mint Oil Microcapsules by Microfluidics with High Efficiency and Controllability in Release Properties. *Microfluid. Nanofluidics* **2020**, *24*, 1–11. [CrossRef]
29. Gouin, S. Microencapsulation: Industrial Appraisal of Existing Technologies and Trends. *Trends Food Sci. Technol.* **2004**, *15*, 330–347. [CrossRef]
30. Wang, X.; Cheng, F.; Wang, X.; Feng, T.; Xia, S.; Zhang, X. Chitosan Decoration Improves the Rapid and Long-Term Antibacterial Activities of Cinnamaldehyde-Loaded Liposomes. *Int. J. Biol. Macromol.* **2021**, *168*, 59–66. [CrossRef]
31. Chen, S.; Zhang, Z.; Wei, X.; Sui, Z.; Geng, J.; Xiao, J.; Huang, D. Antibacterial and Antioxidant Water-Degradable Food Packaging Chitosan Film Prepared from American Cockroach. *Food Biosci.* **2022**, *49*, 101893. [CrossRef]

32. Sargın, İ.; Kaya, M.; Arslan, G.; Baran, T.; Ceter, T. Preparation and Characterisation of Biodegradable Pollen–Chitosan Microcapsules and Its Application in Heavy Metal Removal. *Bioresour. Technol.* **2015**, *177*, 1–7. [CrossRef] [PubMed]
33. Hong, K.H. Preparation and Properties of Multi-Functional Cotton Fabric Treated by Gallnut Extract. *Text. Res. J.* **2014**, *84*, 1138–1146. [CrossRef]
34. Zheng, H.; Li, X.; Liu, L.; Bai, C.; Liu, B.; Liao, H.; Yan, M.; Liu, F.; Han, P.; Zhang, H.; et al. Preparation of Nanofiber Core-Spun Yarn Based on Cellulose Nanowhiskers/Quaternary Ammonium Salts Nanocomposites for Efficient and Durable Antibacterial Textiles. *Compos. Commun.* **2022**, *36*, 101388. [CrossRef]
35. Prabhakar, P.; Sen, R.K.; Patel, M.; Dwivedi, N.; Singh, S.; Kumar, P.; Chouhan, M.; Yadav, A.K.; Mondal, D.P.; Solanki, P.R.; et al. Development of Copper Impregnated Bio-Inspired Hydrophobic Antibacterial Nanocoatings for Textiles. *Colloids Surf. B Biointerfaces* **2022**, *220*, 112913. [CrossRef]
36. Zhou, J.; Wang, Y.; Pan, W.; Xiang, H.; Li, P.; Zhou, Z.; Zhu, M. High Thermal Stability Cu2O@OZrP Micro-Nano Hybrids for Melt-Spun Excellent Antibacterial Activity Polyester Fibers. *J. Mater. Sci. Technol.* **2021**, *81*, 58–66. [CrossRef]
37. Vishwakarma, A.; Singh, M.; Weclawski, B.; Reddy, V.J.; Kandola, B.K.; Manik, G.; Dasari, A.; Chattopadhyay, S. Construction of Hydrophobic Fire Retardant Coating on Cotton Fabric Using a Layer-by-Layer Spray Coating Method. *Int. J. Biol. Macromol.* **2022**, *223*, 1653–1666. [CrossRef]
38. Song, X.; Shi, L.; Liu, S.; Hou, C.; Zhu, K.; Cheng, Q.; Mei, L. Development of Microcapsule Bioactive Paper Loaded with Chinese Fir Essential Oil to Improve the Quality of Strawberries. *Coatings* **2022**, *12*, 254. [CrossRef]
39. İPliKçiOğlu ÇiL, G.; Küplülü, Ö.; CengiZ, G.; Korkmaz, S.D.; Arslan, B.; Gürcan, S. Antibacterial Activity of Turkish Honey against Selected Foodborne Pathogens. *Ank. Üniv. Vet. Fakültesi Derg.* **2020**, *67*, 413–418. [CrossRef]
40. Ngamakeue, N.; Chitprasert, P. Encapsulation of Holy Basil Essential Oil in Gelatin: Effects of Palmitic Acid in Carboxymethyl Cellulose Emulsion Coating on Antioxidant and Antimicrobial Activities. *Food Bioprocess Technol.* **2016**, *9*, 1735–1745. [CrossRef]
41. Kanzler, C.; Haase, P.T.; Schestkowa, H.; Kroh, L.W. Antioxidant Properties of Heterocyclic Intermediates of the Maillard Reaction and Structurally Related Compounds. *J. Agric. Food Chem.* **2016**, *64*, 7829–7837. [CrossRef] [PubMed]
42. Zhou, Y.; Cao, F.; Luo, F.; Lin, Q. Octacosanol and Health Benefits: Biological Functions and Mechanisms of Action. *Food Biosci.* **2022**, *47*, 101632. [CrossRef]
43. do Couto, M.V.S.; da Costa Sousa, N.; Paixão, P.E.G.; dos Santos Medeiros, E.; Abe, H.A.; Meneses, J.O.; Cunha, F.S.; Filho, R.M.N.; de Sousa, R.C.; Maria, A.N.; et al. Is There Antimicrobial Property of Coconut Oil and Lauric Acid against Fish Pathogen? *Aquaculture* **2021**, *545*, 737234. [CrossRef]
44. Ponnusamy, K.; Paul, D.; Kim, Y.S.; Kweon, J.H. 2(5H)-Furanone: A Prospective Strategy for Biofouling-Control in Membrane Biofilm Bacteria by Quorum Sensing Inhibition. Braz. *J. Microbiol.* **2010**, *41*, 227–234. [CrossRef]
45. Lee, A.R.; Han, C.H.; Yi, E. Preparation and Characterization of Melamine-Formaldehyde Microcapsules Containing Citrus Unshiu Essential Oil. *Fibers Polym.* **2014**, *15*, 35–40. [CrossRef]
46. Rezaeinia, H.; Ghorani, B.; Emadzadeh, B.; Tucker, N. Electrohydrodynamic Atomization of Balangu (*Lallemantia Royleana*) Seed Gum for the Fast-Release of *Mentha Longifolia* L. Essential Oil: Characterization of Nano-Capsules and Modeling the Kinetics of Release. *Food Hydrocoll.* **2019**, *93*, 374–385. [CrossRef]
47. Bajac, J.; Nikolovski, B.; Lončarević, I.; Petrović, J.; Bajac, B.; Đurović, S.; Petrović, L. Microencapsulation of Juniper Berry Essential Oil (*Juniperus Communis* L.) by Spray Drying: Microcapsule Characterization and Release Kinetics of the Oil. *Food Hydrocoll.* **2022**, *125*, 107430. [CrossRef]
48. Muskovics, G.; Felföldi, J.; Kovács, E.; Perlaki, R.; Kállay, T. Changes in Physical Properties during Fruit Ripening of Hungarian Sweet Cherry (*Prunus Avium* L.) Cultivars. *Postharvest Biol. Technol.* **2006**, *40*, 56–63. [CrossRef]
49. Duhoranimana, E.; Karangwa, E.; Lai, L.; Xu, X.; Yu, J.; Xia, S.; Zhang, X.; Muhoza, B.; Habinshuti, I. Effect of Sodium Carboxymethyl Cellulose on Complex Coacervates Formation with Gelatin: Coacervates Characterization, Stabilization and Formation Mechanism. *Food Hydrocoll.* **2017**, *69*, 111–120. [CrossRef]
50. Staroszczyk, H.; Sztuka, K.; Wolska, J.; Wojtasz-Pająk, A.; Kołodziejska, I. Interactions of Fish Gelatin and Chitosan in Uncrosslinked and Crosslinked with EDC Films: FT-IR Study. *Spectrochim. Acta Part A Mol. Biomol. Spectrosc.* **2014**, *117*, 707–712. [CrossRef]
51. Ghezal, I.; Moussa, A.; Ben Marzoug, I.; El-Achari, A.; Campagne, C.; Sakli, F. Investigating Waterproofness and Breathability of a Coated Double-Sided Knitted Fabric. *Coatings* **2022**, *12*, 1572. [CrossRef]